ELSEVIER

Journal of Power Sources 63 (1996) 221–234

JOURNAL OF POWER SOURCES

Analytical fuel cell modeling

F. Standaert [a], K. Hemmes [b], N. Woudstra [a]

[a] Laboratory for Thermal Power Engineering (WBMT-EV), Delft University of Technology, PO Box 5037, 2600 GA Delft, The Netherlands
[b] Delft University of Technology, Faculty STM, Rotterdamse weg 137, 2628 AL Delft, The Netherlands

Received 6 June 1996; revised 25 September 1996; accepted 30 September 1996

Abstract

It will be shown that some important characteristics of stationary operating fuel cells can be understood by analyzing a simple basic isothermal cell model. The model is independent of the type of fuel cell and will be used for a general description of cells supplied with gaseous fuel and oxidant. An example is also given in which the results are compared with published data of a bench-scale molten carbonate fuel cell (MCFC). Simple expressions relating the cell voltage, cell current and fuel utilization are derived and found to be accurate despite their simplicity. Deviations in analytically calculated cell voltages from numerical computations are in the order of mV. Moreover, it will be shown that a non-homogeneous current distribution yields an extra overpotential in the order of 10 mV for an MCFC.

Keywords: Fuel cells; Analytical models; Cell voltage; Current density distribution; Fuel utilization

1. Introduction

Engineering aspects often dominate the setup of fuel cell models and make them rather complicated. Therefore, most fuel cell models are not suitable for an analytical approach and require extensive computer software for generating numerical results. In addition, the dependence of fuel cell behaviour on the model parameters is often difficult to express on the basis of numerical results only. The great advantage of an analytical model is that relations between the variables can be made clear in a direct way and that fuel cell performance can be determined by the derivation of analytical expressions. On the other hand, simple mathematical analyses are only possible for highly idealized models. Nevertheless, analytical results are important in the explanation of results obtained from complicated numerical models as well as of empirical relations obtained from measurements. So, despite their limitations, analytical results contribute to a better understanding of fuel cell behaviour.

In this paper, a simple basic fuel cell model is introduced for a rectangular flat plate fuel cell. The objective of the 'basic model' is to provide insight in the elementary characteristics of stationary operating, isothermal fuel cells, using simple mathematics. In the 'basic model' a fuel cell is described as an equivalent electrical circuit (see Fig. 1). This approach is also used in Refs. [1–3] and will be elaborated into more detail in this paper. Special attention will be paid to a linear relation between the cell voltage, the total fuel utilization and the cell current. Although measurements on a bench-scale molten carbonate fuel cell (MCFC) confirm this double linear relation [1], a detailed derivation of the relation is not given in any of the references. In this paper, a detailed derivation will be given and it will be shown that more accurate results are obtained if the relation is slightly adapted.

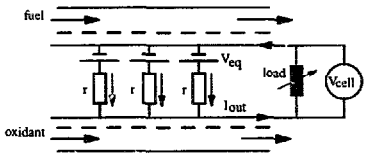

Fig. 1. Representation of a fuel cell as an equivalent electrical circuit.

Table 1 shows the list of assumptions that underlie the setup of the 'basic model'. Oxidant utilization can be taken into account in a similar way as fuel utilization (see Appendix A), but will be neglected for reasons of simplicity. Due to the assumptions 5 and 6, the setup of the 'basic model' is possible without paying special attention to the theory of chemical kinetics. Despite the assumptions listed in Table 1, the 'basic model' can, in most cases, only be 'solved' by using a numerical method. However, it will be shown that linearization of the Nernst potential in the 'basic model' yields an 'analytical cell model', suitable for the derivation of analytical expressions that are in good agreement with numerical computations and measurements.

PII S0378-7753(96)02479-2

Table 1
Overview of the model assumptions

1	Stationary fuel cell (time independent)
2	Isothermal fuel cell
3	Large oxidant flow (negligible oxidant utilization)
4	Changes in fuel composition are significant in the direction of the cell outlet only
5(a)	Local overpotential depends linearly on the local current density through a quasi-ohmic resistance, r
5(b)	Quasi-ohmic resistance, r, is independent of position
6	All reactions in the gas phase are in equilibrium
7	Nernst potential is considered to be independent of hydrostatic pressure gradients

2. Basic isothermal fuel cell model

The total anode surface of the cell is given by BL, where L and B are, respectively, the length and the width of the cell. The approach will be one-dimensional, which means that all variables are considered as a function of the X-coordinate only, i.e. the horizontal distance (Fig. 1) between a cross section of the cell and the cell inlet.

Changes in fuel and oxidant composition occur due to the electrochemical reactions that are taking place inside the cell. Hence, the local equilibrium potential, as given by Nernst law, depends on the local composition of fuel and oxidant. The local overpotential $\eta(X)$ is defined as the difference between the local equilibrium potential (V_{eq}) and the cell potential (V_{cell}) at which the current is delivered. Assumption 5(a) in Table 1 leads to

$$\eta(X) = V_{eq}(X) - V_{cell} = ri(X) \tag{1}$$

This linear current–voltage relation is not evident from a theoretical point of view. The quasi-ohmic resistance, r, does not only account for ohmic losses, but also for voltage losses due to concentration and activation polarization. Eq. (1) is realistic for an MCFC at normal operation, because experimental current–voltage relations are almost perfectly linear for this type of cell (see e.g. [1]). But for low-temperature fuel cells a strong decrease in cell voltage is observed at low current densities, usually ascribed to the activation polarization. Furthermore, at high current densities diffusion limitations occur [4,5]. Nevertheless, the current–voltage relation of a low-temperature cell can be linearized accurately for intermediate current densities, yielding an expression for $\eta(X)$ as $V_{cor} + ri(X)$. Rewriting this expression gives Eq. (1) with an adapted value for $V_{eq}(X)$. Hence, for low-temperature cells, the initial value $V_{eq}(0)$ must be set equal to the open-circuit voltage (OCV) minus the correction term V_{cor}.

Note that the resistance of the current collectors is assumed to be negligible in the definition of the overpotential η in Eq. (1), so that the voltage between two current collectors is equal to V_{cell} throughout the cell. For reasons of simplicity, we assume also that the quasi-ohmic resistance is uniform, i.e. $r(X) = r$ for all X. In most cases, the quasi ohmic resistance depends on temperature mainly and, hence, this simplification is a direct consequence of the assumption that the fuel cell is isothermal. In general, electrode polarization depends also on the local gas compositions, thus on X. But in this paper we will also neglect this influence, which is often of secondary importance.

Below we will introduce an ordinary differential equation (ODE) for the fuel utilization, u, based on the expression for the overpotential given in Eq. (1). The equilibrium potential V_{eq} will appear in this ODE as a function of u and not as a function of X. In fact, the equilibrium potential depends mainly on the local fuel and oxidant composition and is practically independent of the small total pressure gradients in the process flows [4]. Neglecting hydrostatic pressure gradients it is possible to determine the composition of the process flows as a function of the fuel utilization, u. The Nernst equation gives thus the local equilibrium potential in terms of the utilization $u(X)$.

For reasons of simplicity, we assume a large flow of oxidant being considered as homogeneous. Thus, we have to take into account the utilization of fuel only. It is convenient to represent the maximum amount of current, that is produced in the hypothetical situation of complete fuel utilization, by I_{in}, which we will call the 'equivalent input current'. Note that I_{in} can be calculated from the gas composition and the gas flow rate, using Faraday's law. The delivered current is denoted by I_{out} and will be smaller than the equivalent input current I_{in}. The ratio I_{out}/I_{in} gives the total fuel utilization and, in an analogous way, the local fuel utilization $u(X)$ is defined as the fraction of I_{in} generated in the area between the cell inlet and position X

$$u(X) = \frac{B}{I_{in}} \int_0^X i(\zeta)\, \mathrm{d}\zeta, \quad (0 \le u \le 1) \tag{2}$$

where B is the width of the cell. The expression for the overpotential in Eq. (1) can be used to eliminate the local current density i in Eq. (2). Differentiating the result with respect to X and writing $V_{eq}(u)$ instead of $V_{eq}(X)$ we obtain the following ordinary differential equation

$$\frac{\mathrm{d}u}{\mathrm{d}X} = \frac{B}{rI_{in}}(V_{eq}(u) - V_{cell}), \quad (0 < X < L) \tag{3}$$

From the definition of the utilization u in Eq. (2) it follows that u is zero at the cell inlet, i.e. for $X = 0$. Apart from this initial value for u, the ODE must be supplied with either a suitable end value for u or a value for V_{cell}. Choosing the first possibility, i.e. imposing an end value u_1 for the utilization, we have to solve Eq. (3) for $u(X)$ and V_{cell}, taking into account the boundary conditions

$$u(0) = 0, \quad u(L) = u_1, \quad (0 < u_1 < 1) \tag{4}$$

In order to facilitate the evaluation of the results, it is convenient to scale Eqs. (3) and (4). To this end, we successively relate the equivalent input current I_{in} to the cell surface BL and the space coordinate X to the cell length L. The scaled variables are denoted by i_{in} and x respectively

$$i_{in}=\frac{I_{in}}{BL},\quad x=\frac{X}{L},\quad (0<x<1) \tag{5}$$

Scaling Eqs. (3) and (4), by using these scaled variables, we obtain the following boundary value problem (BVP)

$$\begin{cases}\dfrac{du}{dx}=\dfrac{1}{ri_{in}}(V_{eq}(u)-V_{cell}), & (0<x<1)\\ u(0)=0, & u(1)=u_1=I_{out}/I_{in}\end{cases}$$

In this BVP the first-order differential equation for the utilization is supplied with two boundary conditions. This implies that the solution of the BVP is twofold, i.e. is given by the set $(u(x), V_{cell})$. This solution depends on the product ri_{in} rather than on the individual data for r and i_{in}. However, the local current density does depend on these individual data, e.g. the average current density over the whole cell is equal to $i_{in}u_1$.

Once the BVP has been solved, the local current density i can be calculated from

$$i(x)=i_{in}\frac{du}{dx}(x),\quad (0<x<1) \tag{6}$$

Note that the individual values for $V_{eq}(0)$ and V_{cell} are irrelevant, because only the overpotential $(V_{eq}(u)-V_{cell})$ appears in the BVP. Hence, the difference $V_{eq}(0)-V_{cell}$ is important; it is this difference rather than the individual terms that influence the local current density i and the local fuel utilization u.

In this paper, the 'basic model' is only used to calculate the electrical variables, i.e. the current density, i, the fuel utilization, $u(x)$, and the cell voltage V_{cell}. We distinguish this set of variables from the set of so-called hydrodynamical variables. In fluid dynamics the term hydrodynamical variables refers to the hydrostatic pressure, the fluid density and the velocity of a fluid flow. In a fuel cell model, the calculation of hydrodynamical variables requires a detailed description of the configuration of the gas channels. However, as long as sufficient gas flow is allowed for, these details appear to be irrelevant for the calculation of the variables i, u and V_{cell}, within the 'basic model'.

Solving the BVP requires an expression for the local equilibrium potential in terms of the utilization u. To obtain an expression for $V_{eq}(u)$ we simply assume fuel and oxidant to be a mixture of ideal gases and neglect concentration gradients over a cross section of a gas channel (ideal mixing in the gas phase).

3. The linearized Nernst potential for a 'basic MCFC model'

In this section the general 'basic model' is specified for an MCFC. This requires the representation of the equilibrium potential inside an MCFC as a function of the fuel utilization u. Oxidant utilization in an MCFC is often sufficient low to have little overall effect [6], because in practice large oxidant flows are used for cooling. Therefore and for reasons of simplicity, it is convenient to neglect oxidant utilization in the 'basic MCFC model'. The representation of the equilibrium potential $V_{eq}(u)$ inside an MCFC for zero oxidant utilization is derived in Appendix A, assuming temperature and pressure to be uniform. Furthermore, we do not consider the methane reforming reaction and assume that the water–gas shift reaction is in equilibrium. The expression resulting for $V_{eq}(u)$ turns out to be complicated and unsuitable for analytical purposes; it can be used in numerical computations, whose results are given in the next sections. In order to make a simple mathematical analysis of the 'basic model' possible, a linear approximation for the equilibrium potential will be derived below.

The Nernst law gives the equilibrium potential in terms of partial pressures p_i of the species in the process flows

$$V_{eq}(u)=E^0+\frac{RT}{2F}\ln(pO_2^{1/2}pCO_2^c)+\frac{RT}{2F}\ln\frac{pH_2}{pCO_2^a pH_2O} \tag{7}$$

where E^0 is determined by thermodynamics and the superscripts 'a' or 'c' refer, respectively, to the anode or cathode gas composition. As we assume a homogeneous cathode flow, the second term on the right-hand side of Eq. (7) is considered to be independent of position. In Appendix A it is shown how the partial pressures in the last term of Eq. (7) can be expressed in terms of the fuel utilization u.

At 650 °C the factor $RT/2F$ in the Nernst equation is equal to about 40 mV, which is small in comparison with common values for the OCV (typical 1000 mV). The Nernst potential $V_{eq}(u)$ in Eq. (7) varies thus moderately with u, except if any of the partial pressures in the last logarithmic term is very low. The shift reaction will not cause extreme low partial pressures due to its equilibrium state. So, only for values of u near zero or unity we may expect big changes in the logarithmic term. Nevertheless, Fig. 2 shows that for most values of u, an accurate approximation $V_{eq}^*(u)$ for the local equilibrium potential $V_{eq}(u)$ can be obtained from a linearization

$$V_{eq}^*(u)=V_{eq}^*(0)-\alpha u,$$

$$\alpha=\text{constant}\approx-\frac{dV_{eq}}{du}\text{ for most }u\in(0,1) \tag{8}$$

The constant of proportion α in the linearized equilibrium potential is not exactly defined, but must be a characteristic value for the derivative of $-V_{eq}(u)$ with respect to u. Note that the dimension of α is V, since u is dimensionless.

As shown in Fig. 2, the local equilibrium potential $V_{eq}(u)$ inside an MCFC contains an initial dip near the origin, i.e. the equilibrium potential decreases more rapidly near $u=0$ than in the neighborhood of $u=1/2$. Moreover, the equilibrium potential also decreases fast near the point of singularity $u=1$. Apparently, a suitable value for α is obtained if the derivative of the equilibrium potential is determined in the point of inflection, i.e. the point, say u^*, where the second

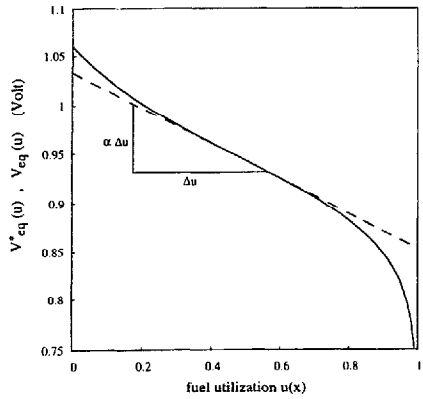

Fig. 2. Example of a linearized Nernst equation $V^*_{eq}(u)$ in case of an MCFC. Note the initial dip in the exact Nernst equation $V_{eq}(u)$ at low utilization. (– – –) $(V^*_{eq}(u)$, and (——) $V_{eq}(u)$; for parameter values see Table 2.

derivative of the equilibrium potential with respect to u is zero. Then we have

$$\frac{d^2V_{eq}}{du^2}(u^*)=0, \quad \frac{dV_{eq}}{du}(u^*)=-\alpha,$$

$$V^*_{eq}(0)=V_{eq}(u^*)+\alpha u^* \tag{8a}$$

For instance, consider the inlet fuel composition presented in Table 2 and a homogeneous cathode flow of 70% air and 30% CO_2. In Table 2 the mole fractions after equilibrium are based on a value of $K=0.5$ for the equilibrium constant of the reverse shift reaction (corresponding to a cell temperature of 650 °C and atmospheric pressure [7]). For the fuel composition presented in Table 2, the point of inflection of the function $V_{eq}(u)$ can be determined numerically to be $u^*=0.50$. In this point the slope of $V_{eq}(u)$ is 0.18 V. Hence in this case the linear approximation for the equilibrium potential is given by

$$V^*_{eq}(u)=1.03-0.18u, \quad (0.2\le u\le 0.8) \tag{9}$$

where the actual OCV for this gas composition is 1.06 V. Because of the initial dip in the Nernst potential, the value of $V^*_{eq}(0)$ is 30 mV lower than the actual OCV. The boundaries for u given in Eq. (9) are not strict, but give an idea of the interval for which the linear approximation is accurate.

If the local equilibrium potential of a low-temperature cell is linearized, then the difference $V^*_{eq}(0)-V_{eq}(0)$ must not be confused with the correction term V_{cor} that was introduced in the previous section.

Machielse [1] determined experimentally the quasi-ohmic resistance r for an MCFC to be 1.195 Ω cm², see Table 2. He also applied the PSI (Physical Sciences Inc.) cell model [8] for his experimental conditions and obtained a 10% lower value of 1.08 Ω cm². Throughout this paper we will use $r=1.08$ Ω cm². Only in Section 5, where a comparison is made with the experimental results obtained by Machielse, we will use $r=1.195$ Ω cm².

4. Analytical solutions of the 'basic model'

The BVP that was introduced in Section 2 can only be solved in closed form for some simplified versions of the equilibrium potential $V_{eq}(u)$. In this section an analytical solution of the BVP is derived, assuming the function $V_{eq}(u)$ to be linear. In Section 3 it was shown for an MCFC that $V_{eq}(u)$ is almost linear up to high values for the fuel utilization u. The analytical solution will be thus fairly accurate up to high values for the total fuel utilization u_t. The obtained analytical expressions will therefore apply to problems with practical values for u_t.

Also approximate solutions for the BVP will be derived and in Section 4.2 the influence of the initial dip in the equilibrium potential $V_{eq}(u)$ will be considered.

4.1. Analytical cell model

The cell model that is obtained if a linear function is used to describe the equilibrium potential $V_{eq}(u)$ in the BVP is referred to as the 'analytical cell model'. The problem is to find a function u: $[0,1]\rightarrow[0,u_t]$ and a constant V^*_{cell} satisfying

Table 2
Standard gas compositions for an MCFC and corresponding parameter values at atmospheric pressure; PSI = calculated from PSI model [1], exp. = determined from experimental results [1]. (Methane reforming equilibrium is neglected.)

Anode inlet gas	H_2	CO	H_2O	CO_2	CH_4
Before equilibrium	0.64	0	0.20	0.16	0
After equilibrium	0.56	0.08	0.28	0.08	0
Cathode inlet gas	air			CO_2	
Homogeneous	0.70			0.30	
T (°C)	α (V)	$V^*_{eq}(0)$ (V)	$V_{eq}(0)$ (V)	K	r (Ω cm²)
650	0.18	1.03	1.06	0.5	1.08 (PSI)
					1.195 (exp.)

$$\begin{cases} \dfrac{du}{dx} = \dfrac{1}{ri_{in}}(V^*_{eq}(0) - \alpha u - V^*_{cell}), & (0 < x < 1) \\ u(0) = 0, & u(1) = u_1 \end{cases}$$

where α (defined by Eq. (8)) and ri_{in} are positive constants.

Integration of the differential equation with respect to x from zero to a point in the interval [0,1] gives

$$u(x) = \frac{V^*_{eq}(0) - V^*_{cell}}{\alpha}\left(1 - \exp\left(\frac{-\alpha x}{ri_{in}}\right)\right) \quad (10)$$

This function must satisfy the end condition $u(1) = u_1$. Using this condition, the following relation between V^*_{cell} and u_1 can be derived

$$V^*_{cell} = V^*_{eq}(0) - \alpha\left(1 - \exp\left(\frac{-\alpha}{ri_{in}}\right)\right)^{-1} u_1 \quad (11)$$

The set $(u(x), V^*_{cell})$ given by Eqs. (10) and (11) is the solution of the Analytical Cell Model. The local current density inside the cell can be calculated from this analytical solution, using Eq. (6):

$$i(x) = i_{in}\frac{du}{dx} = \frac{V^*_{eq}(0) - V^*_{cell}}{r}\exp\left(-\frac{\alpha}{ri_{in}}x\right) \quad (0 < x < 1) \quad (12)$$

Note that Eq. (11) is linear with respect to the total utilization u_1. Thus, the use of a linearized Nernst equation results in an expression for the cell voltage that shows a linear dependence on u_1. In the following an approximation for V^*_{cell} will be derived that is linear with respect to the total utilization u_1 as well as to the average current density $i_{in}u_1$. We start the derivation of this double linear expression for V^*_{cell} with the introduction of two more relations, i.e. a relation between $i(0)$ and $i(1)$ and a relation between the cell voltage and the electrical losses due to the quasi-ohmic resistance, r.

According to Eq. (12) the following identity holds

$$i(1) - i(0) = \frac{V^*_{eq}(0) - V^*_{cell}}{r}\left(\exp\left(-\frac{\alpha}{ri_{in}}\right) - 1\right)$$

The cell voltage V^*_{cell} can be eliminated from this identity, using Eq. (11). Then the following simple relation between the current density $i(0)$ at the cell inlet and the current density $i(1)$ at the cell outlet is obtained

$$i(1) - i(0) = -\frac{\alpha u_1}{r} \quad (13)$$

In order to obtain a relation between the cell voltage and the quasi-ohmic losses we multiply both sides of the differential equation in the analytical cell model by du/dx and integrate with respect to x from zero to unity

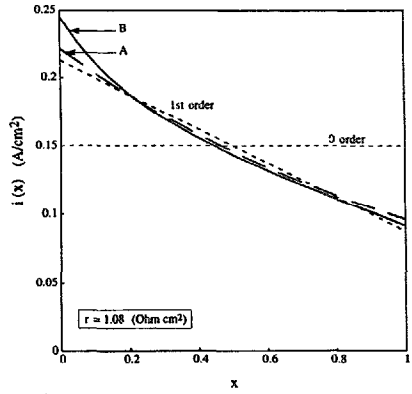

Fig. 3. Current distribution inside an MCFC: according to (curve A) the 'analytical cell model', and (curve B) numerical computations based on the non-linearized Nernst equation are shown. Also the constant (zero-order) and linearly decreasing (first-order) approximation.

$$\int_0^1 \left(\frac{du}{dx}\right)^2 dx = \frac{1}{ri_{in}}\int_0^{u_1}(V^*_{eq}(0) - \alpha u - V^*_{cell})\,du$$

$$= \frac{1}{ri_{in}}\left(V^*_{eq}(0) - \frac{1}{2}\alpha u_1 - V^*_{cell}\right)u_1$$

Rewriting this result, using the first part of Eq. (12) and the following definition of the average current density i_{out}

$$i_{out} = i_{in}u_1 \quad (14)$$

we obtain

$$V^*_{cell} = V^*_{eq}(0) - \frac{1}{2}\alpha u_1 - \frac{r}{i_{out}}\int_0^1 i^2(x)\,dx \quad (15)$$

Note that Eq. (15) is exact within the analytical cell model. This equation states that the cell voltage is equal to the average value of the linearized equilibrium potential inside the cell, minus the total loss in cell voltage due to the quasi-ohmic resistance r.

It is possible to calculate the integral in Eq. (15) by using the exponential relation for the local current density $i(x)$ given by Eq. (12). However, this is not very practical since the expression for the cell voltage, obtained in this way, will be equivalent to the expression for V^*_{cell} given in Eq. (11). Although the exact current distribution is known to be exponential, it is convenient to approximate the current density $i(x)$ in the last term of Eq. (15) in order to obtain approximate expressions for the cell voltage that are more simple than the exact expression in Eq. (11). To this end, we assume $i(x)$ either to be constant (zero-order approximation) or to be linearly decreasing (first-order approximation). The approximate current distributions must have the same average

current density i_{out} as the exact (i.e. the exponential) current distribution (see Fig. 3).

Note that the integral in Eq. (15) is equal to the average value of i^2 over the whole cell, which is always greater than or equal to the square of the average current density, i.e. i_{out}^2 (from the Lemma of Cauchy–Schwarz [9]). This means that the last term in Eq. (15), that represents the total loss in cell voltage due to the quasi-ohmic resistance, r, is minimum for a homogeneous current distribution

$$\frac{r}{i_{out}}\int_0^1 i^2(x)\,dx \geq r i_{out} \tag{16}$$

where the equality holds if (and only if) the current density $i(x)$ is equal to the average current density i_{out} for all x. An upper bound for the cell voltage V_{cell}^* is thus obtained if we assume a homogeneous current distribution, $i(x) \equiv i_{out}$, in order to approximate the integral in Eq. (15). Then the zero-order approximation for the cell voltage V_{cell}^* is obtained. This approximation does not account for the overpotential, say A_1, due to the non-homogeneity of the current distribution

$$V_{cell}^* = V_{eq}^*(0) - \frac{1}{2}\alpha u_1 - r i_{out} - A_1,$$

$$A_1 = 0 \text{ in zero-order approximation} \tag{17}$$

where $A_1 \geq 0$ can be omitted in order to obtain the double linear, zero-order approximation for V_{cell}^*. This double linear relation for the cell voltage was also derived by Machielse [1] and Hemmes [2], using, however, different assumptions and approximations. The second term on the right-hand side of Eq. (17) is called the Nernst loss and is the direct consequence of the decrease in $V_{eq}^*(u)$ in the direction of the cell outlet. The term ri_{out} represents the loss in cell voltage due to the quasi-ohmic resistance, r, in the case of a homogeneous current distribution. Furthermore, we have shown that A_1 is the extra overpotential due to the non-homogeneity of the current distribution inside the cell.

Another possibility is the use of a linear or first-order approximation for the local current density. According to the identity in Eq. (13) this means that $i(x)$ is approximated by

$$i(x) \approx i_{out} + \frac{\alpha u_1}{r}\left(\frac{1}{2} - x\right), \quad \text{first-order approximation}$$

Note that in this first-order approximation, the average current density is still equal to i_{out}. Using the first-order approximation for the local current density to approximate the integral in Eq. (15), we obtain the following expression for V_{cell}^*

$$V_{cell}^* = V_{eq}^*(0) - \frac{1}{2}\alpha u_1 - r i_{out} - \frac{1}{3}Z^2 r i_{out} + A_2,$$

$$A_2 = 0 \text{ in first-order approximation} \tag{18}$$

where A_2 is the inaccuracy in the first-order approximation and the dimensionless number Z is defined by

$$Z = \frac{\alpha}{2 r i_{in}} \geq 0 \tag{19}$$

The significance of the number Z will be explained in Section 6.

Comparing Eqs. (17) and (18) we find that the extra overpotential A_1 due to the non-homogeneity of the current distribution inside the cell is given by

$$A_1 = \frac{1}{3}Z^2 r i_{out} - A_2,$$

$$A_2 = 0 \text{ in first-order approximation} \tag{20}$$

Although the first-order approximation is not exact, it will turn out that the expression in Eq. (20) with $A_2 = 0$ is very close to the exact value of A_1.

Furthermore, it will be illustrated by an example that the obtained approximations for V_{cell}^* are accurate, notwithstanding the fact that simple estimations for the local current density were used in the derivations. Note that, once V_{cell}^* has been calculated using one of the Eqs. (17), (18) or (11), based on the zero- or first-order approximation for the local current density or the exact solution, respectively, a more accurate expression for the local current density can be obtained from Eq. (12).

We consider the MCFC as an example. For an MCFC typical values for $V_{eq}^*(0)$, α and r are $V_{eq}^*(0) = 1.03$ V, $\alpha = 180$ mV and $r = 1.08\ \Omega\,cm^2$, respectively. The equivalent input current i_{in} is assumed to be 200 mA/cm^2. At a total utilization of $u_1 = 0.75$, the average current density is equal to 150 mA/cm^2, which is a standard value for an MCFC operation. Within the analytical cell model the cell voltage V_{cell}^* can be calculated exactly from Eq. (11) to be 0.7912 V. The zero-order approximation in Eq. (17) gives an upper bound which is 9.3 mV larger, i.e. $V_{cell}^* = 0.8005 - A_1$ V. This means that we have an extra decrease in cell voltage of 9.3 mV due to a non-homogeneous current distribution. The first-order approximations in Eqs. (18) and (20) turn out to be very accurate. Eq. (18) with $A_2 = 0$ yields a cell voltage of 0.7911 V compared with 0.7912 V for the exact solution. Hence, A_2 is, in fact, in the order of 0.1 mV, which is negligibly small.

Fig. 3 shows the current distribution, obtained from Eq. (12) as well as from numerical computations based on the non-linearized Nernst equation. As a consequence of the initial dip in the Nernst potential (see Fig. 2 for small values of the local fuel utilization) the analytically calculated current distribution shows a much smaller current density near the cell inlet, compared with the numerically calculated current distribution. This implies that the analytically calculated current density will be somewhat larger in other parts of the cell, since the average current density was set equal for both current distributions.

For the MCFC example ($u_1 = 0.75$), the extra losses in cell voltage due to the non-homogeneity of the current distribution are small (in the order of 10 mV). More general,

but still within the assumptions of the 'basic model', we can conclude that at normal (high efficient) operation, the extra electrical losses due to a non-homogeneous current distribution inside an isothermal fuel cell are small and will be close to the estimation $(Z^2/3)ri_{out}$ given by Eq. (20).

4.2. Extended analytical cell model

In this section we will consider the influence of the initial dip in the Nernst equation on the cell voltage. To this end, we will use a partly linearized equilibrium potential, instead of $V^*_{eq}(u)$. In the so-called 'extended analytical cell model' we consider the local equilibrium potential to be given by $V_{eq}(u)$ for $u < u^*$ and $V^*_{eq}(u)$ for $u > u^*$, i.e. the function that follows the exact Nernst equation up to the point of inflection u^* (see Eq. (8a)) and then connects with the linear approximation $V^*_{eq}(u)$ as used in the analytical cell model.

It is shown in Appendix B that the cell voltage V^{ext}_{cell} corresponding with this partly linearized Nernst equation can be approximated by

$$V^{ext}_{cell} \approx V^*_{eq}(0) - \frac{1}{2}\alpha u_l - ri_{out} + C\frac{1}{u_l},$$

$u_l \neq 0$, zero-order approximation (21)

$$V^{ext}_{cell} = V^*_{eq}(0) - \frac{1}{2}\alpha u_l - \left(1 + \frac{1}{3}Z^2\right)ri_{out} + C\frac{1}{u_l},$$

$u_l \neq 0$, first-order approximation (22)

with the constant C equal to the surface between the linear approximation $V^*_{eq}(u)$ and the initial dip in $V_{eq}(u)$. Again the zero- and first-order approximations refer, respectively, to a constant and linearly decreasing current density $i(x)$. Comparing the approximations for V^*_{cell} and V^{ext}_{cell}, we see that the influence of the initial dip in the Nernst equation on the cell voltage can be taken into account by an extra term, i.e. C/u_l.

In the following example it is made clear that V^{ext}_{cell} is a very accurate approximation for the cell voltage V_{cell}, i.e. the cell voltage corresponding with the non-linearized Nernst equation. At least, as shown in Appendix B, for values of u_l in the interval for which the linear fit of the equilibrium potential is accurate (see Section 3)

$$V_{cell} \approx V^{ext}_{cell}, \quad 0.2 \leq u_l \leq 0.8$$

The accuracy of both approximations in Eqs. (21) and (22) will be illustrated on the basis of a similar MCFC example as was introduced at the end of Section 4.1. However, we now consider different values for i_{in} and u_l, keeping the average current density $i_{out} = i_{in}u_l$ constant at 150 mA/cm^2. For the fuel composition as presented in Table 2, the value of C was numerically determined to be $C = 3$ mV. Fig. 4 shows the cell voltage as a function of the total fuel utilization, u_l, for a constant average current density $i_{out} = 150$ mA/cm^2, according to the zero-order approximation in Eq. (21) as well as to the first-order approximation in Eq. (22). The difference between these two approximations represents the extra loss in cell voltage due to the non-homogeneity of the current distribution.

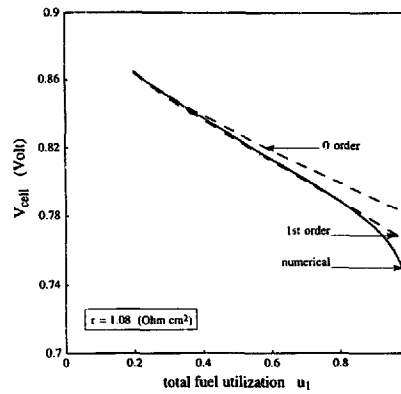

Fig. 4. Example of the cell voltage of an MCFC as a function of the total fuel utilization, u_l, for a constant average current density of 150 mA/cm^2. Top, middle and bottom curves correspond with the zero-order approximation in Eq. (21), the first-order approximation in Eq. (22) and numerical computations, respectively.

The results of numerical computations based on the non-linearized Nernst equation are also plotted in Fig. 4. The approximations appear to be accurate up to a total fuel utilization of 80%. For values of u_l larger than 0.8 the linearization of the Nernst equation fails and the approximations start deviating.

5. Comparison of the models with measurements

In the preceding sections a 'basic model' suitable for a numerical approach and an 'analytical cell model' have been introduced. In this section, some results obtained from these models will be compared with experimental results presented by Machielse [1]. This comparison is mainly directed on the cell voltage of an MCFC as a function of the fuel utilization, in particular on the following identity derived from the Eqs. (22), (14) and (19)

$$\left(\frac{\partial V_{cell}}{\partial u_l}\right)_{i_{out}} \approx -\frac{1}{2}\alpha - \frac{\alpha^2}{6ri_{out}}u_l - C\frac{1}{u_l^2}, \quad u_l \neq 0 \qquad (23)$$

where the index indicates that the partial derivative holds for constant values of the average current density (i_{out} = constant). It will be made clear that this derivative is almost constant for nearly all relevant values of u_l. It strongly determines the relation between the cell voltage and the total fuel utilization u_l.

The conditions outlined in Section 3 are the same as used by Machielse. The values $\alpha = 180$ mV, $C = 3$ mV and

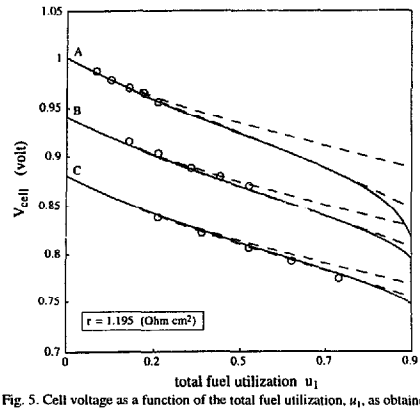

Fig. 5. Cell voltage as a function of the total fuel utilization, u_1, as obtained from experimental results (marked points) on an MCFC bench-scale cell, imposing constant average current densities: (A) 50 mA/cm²; (B) 100 mA/cm², and (C) 150 mA/cm². (– – –) Plots for values of $u_1 \geq 0.2$ only, represent analytical results obtained from Eqs. (21) (top) and (22) (bottom). (———) Numerical results are plotted for all values of $u_1 < 0.9$.

$r = 1.195\ \Omega\ \text{cm}^2$ will thus be used in the calculations. For an average current density of 150 mA/cm² the three terms on the right-hand side of Eq. (23) are successively -90, -15 and -12 mV for $u_1 = 1/2$, the first term being dominant. (Note that this term is independent of u_1, whereas the two small terms in the expression for the derivative are not.) Nevertheless, the sum of the terms appears to be approximately constant for a wide range of values for u_1, as is clear from the almost linear curves in Fig. 4. Calculating the average value of the derivative in Eq. (23) over the interval from $u_1 = 0.2$ to $u_1 = 0.8$, we find

$$\left(\frac{\partial V_{cell}}{\partial u_1}\right)_{i_{out}} \approx -124\ \text{mV}, \quad \text{analytical; } i_{out} = 150\ \text{mA/cm}^2$$

This value will be compared with experimental data obtained by Machielse [1]. His experiments were carried out on an isothermal 1000 cm² MCFC bench-scale cell.

Machielse determined the cell voltage as a function of the total fuel utilization, imposing constant average current densities. The results are reproduced, with permission, in Fig. 5. This figure shows three sets of experimental results, each for a constant average current density. As can be seen, the experimental results within a set can be connected by an almost straight line, from which we could determine

$$\left(\frac{\partial V_{cell}}{\partial u_1}\right)_{i_{out}} \approx -125 \text{ to } -175\ \text{mV}, \quad \text{experimental}$$

where the exact value of the derivative depends on the imposed value of i_{out}. Unfortunately, these values are not given in Ref. [1]. However, the vertical distances in Fig. 5 between two sets of measurements are proportional to the current differences, because of the term ri_{out} in the analytical approximations in Eqs. (21) and (22) (dashed curves). Thus, the average current density i_{out} varies considerably for the three sets of measurements and in accordance with the analytical relation in Eq. (23), the slope of a line through a set of experimental points depends on the imposed value of i_{out}. As the bottom set of experimental points in Fig. 5 yields a slope of approximately -125 mV, very close to the analytical value, it is most likely that this set corresponds to an average current density $i_{out} \approx 150\ \text{mA/cm}^2$.

For a more detailed comparison of the experimental results obtained by Machielse and the theoretical results obtained from either the basic model (numerical computations) or the extended analytical cell model, we assumed that the measurements were carried out for average current densities of 50, 100 and 150 mA/cm². For these current densities the corresponding analytical and numerical results were presented in Fig. 5 together with the experimental results. As shown by this figure, the experimental and theoretical results are in very good agreement.

6. Derivation of input–output relations

As already remarked in the introduction, an analytical approach can contribute to a better understanding of fuel cell behaviour. To this end, some input–output relations will be derived in this section, i.e. fuel cell performance will be expressed in terms of independent variables.

Since the constant of proportion α in the linearized Nernst equation can be determined from the fuel composition (see Section 3), only two independent variables appear in the mathematical formulation of the analytical cell model, i.e. i_{in} and u_1 (see Section 4.1). However, in practice, the two 'control knobs' or independent variables that govern the performance of an isothermal fuel cell are the external load resistance R_{load} and the equivalent input current density i_{in}. Recall that i_{in} can be calculated from Faraday's law. For smaller test cells one can connect an electronic load that keeps the cell voltage or total cell current at a constant value (potentiostatic or galvanostatic control, respectively).

When the pair (R_{load}, i_{in}) is considered as the set of independent variables, instead of (u_1, i_{in}), it is convenient to write the cell voltage as the product of the load resistance and the cell current I_{out}. Relating the load resistance to the cell surface BL we then obtain

$$V^*_{cell} = R_{load} I_{out} = BLR_{load} i_{out} \tag{24}$$

On the other hand, the cell voltage V^*_{cell}, in the zero-order approximation, is given by Eq. (17). Eliminating the cell voltage we find, upon rearrangement

$$i_{out} \approx V^*_{eq}(0) \Big/ \left(BLR_{load} + r + \frac{\alpha}{2i_{in}}\right),$$

zero-order approximation (25)

This current input–output relation gives the average current density i_{out} as a function of the 'two control knobs', R_{load} and i_{in}.

Eq. (25) looks like Ohm's law and contains three 'resistances', all having the dimension $\Omega\ m^2$: the scaled external load resistance, the internal cell resistance, r, and a term $\alpha/(2i_{in})$ that we call 'the utilization resistance'. The utilization resistance is due to the Nernst loss and decreases as the fuel flow increases. (It vanishes in the limiting case of an infinitely large fuel flow, in accordance with the fact that in that case fuel utilization is effectively zero; so achieving, for a fixed R_{load}, the maximum output current i_{max}. (The fuel composition is the same throughout the cell and a homogeneous current distribution is established.) In this limiting case the zero-order approximation is exact and yields

$$i_{max} = V^*_{eq}(0)/(BLR_{load} + r)$$

Recalling Eq. (19) we see that the dimensionless number Z was actually defined as the ratio of two resistances, i.e. the utilization resistance $\alpha/(2i_{in})$ and the quasi-ohmic resistance, r. Below it will be made clear that it is the number Z that largely determines input–output relations of fuel cells.

To obtain the output current density as a function of the cell voltage and the number Z we solve the zero-order approximation in Eq. (17) for u_1 and multiply the obtained equation by i_{in}

$$i_{out} \approx \frac{V^*_{eq}(0) - V^*_{cell}}{ri_{in} + (\alpha/2)}\, i_{in}$$

$$= \frac{V^*_{eq}(0) - V^*_{cell}}{(1+Z)r}, \quad \text{zero-order approximation} \qquad (26)$$

Multiplying Eq. (26) by V^*_{cell} we obtain the power output $p_{out} = i_{out}V^*_{cell}$ per unit cell surface

$$p_{out} \approx \frac{V^*_{eq}(0) - V^*_{cell}}{(1+Z)r} V^*_{cell}, \quad \text{zero-order approximation} \qquad (27)$$

Note that p_{out} as a function of V_{cell} is a parabola with its maximum at $V^*_{cell} = V^*_{eq}(0)/2$. In Fig. 6 the parabolas for $Z = 0$ and $Z = 0.5$ (i.e. for constant i_{in}) are shown. The output power at constant utilization is given by the equation that is obtained if the following identity is substituted into Eq. (27)

$$Z = u_1/\left(\frac{2}{\alpha}(V^*_{eq}(0) - V^*_{cell}) - u_1\right)$$

This latter identity easily follows from Eq. (26), using $i_{out} = i_{in}u_1 = u_1\alpha/(2Zr)$.

Maximum power output means minimum capital costs for fuel cell stacks. Consequently, one may be tempted to operate a fuel cell at a cell voltage $V^*_{cell} = V^*_{eq}(0)/2$ and a fuel utilization u_1, corresponding with the maximum of a parabola in Fig. 6. However from Eqs. (24) and (25) it can be shown, by elimination of i_{out}, that at this point $BLR_{load} = r + (\alpha/2i_{in}) = (1+Z)r$. Hence, the power loss due to internal heat production by the quasi-ohmic resistance, r, is $1/(1+Z)$ times the delivered power in the form of electricity, which is undesirably high. Typical values for an MCFC at normal (high efficient) operation are $Z \approx 0.5$ and $V^*_{cell} = 0.8$ V. Then it follows from Eq. (27) that the output power density p_{out} can increase by 50% for $Z \to 0$, i.e. for $i_{in} \to \infty$, even at constant cell voltage. A further increase in power output can be achieved by decreasing the cell voltage by lowering R_{load}. Fig. 6 shows that for small Z and for a cell voltage equal to half the value of the OCV, a total increase of 100%, respect to typical operation, in power output occurs (i.e. from 0.11 to 0.2–0.25 W/cm^2). However, at these conditions $BLR_{load} \approx r$, which is clearly not an optimum situation for fuel cell operation.

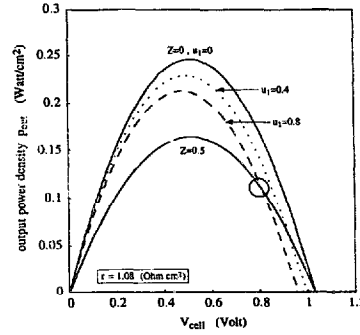

Fig. 6. Power output as a function of the cell voltage for constant values of i_{in}, hence of Z, as well as for constant values of u_1. The circle denotes the neighborhood of normal operation; for parameter values see Table 2.

More accurate input–output relations can be obtained in a similar way, using the first-order approximation in Eq. (22). For instance, analogous to the derivation of Eq. (25) it can be shown that

$$i_{out} \approx \left[V^*_{eq}(0)/\left(BLR_{load} + \left(1 + \frac{1}{3}Z^2\right)r + \frac{\alpha}{2i_{in}}\right)\right] + \frac{Ci_{in}}{V^*_{eq}(0)} \quad u_1 \neq 0; \text{ first-order approximation} \qquad (28)$$

Below we will successively consider examples of the current–input output Eqs. (25) and (28), assuming a fixed load resistance. Examples of i_{out} as a function of R_{load} for a fixed equivalent input current i_{in} are given in Ref. [10].

In Fig. 7 the delivered current of an MCFC as given by Eq. (25), is plotted as a function of the variable i_{in} for a constant (and small) load resistace $BLR_{load} = 4\ \Omega\ cm^2$. Again the same parameter values, listed in Table 2, have been used.

Note that in Fig. 7, the slope of a line connecting a point on the curve and the origin yields the total utilization $u_1 = i_{out}/i_{in}$ as indicated in the figure. Recall that the maximum output current density i_{max} is achieved for an infinitely large value of i_{in}. Imagine that, starting from the point for which $i_{in} = 0.8$

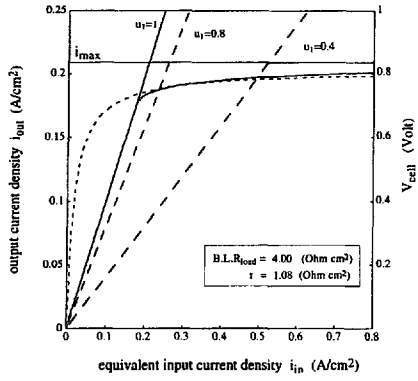

Fig. 7. Output current density as a function of the equivalent input current density for an MCFC at a constant load resistance. (– – –) representing the zero-order approximation in Eq. (25), and (———) according to numerical computations. Lines of constant utilization and the maximum achievable current, based on an OCV of $V_{oc}(0) = 1.06$ V, are also shown.

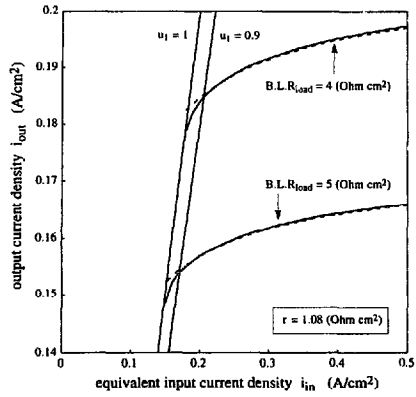

Fig. 8. Close-up of the output current density as a function of the equivalent input current density for an MCFC, showing very good agreement between (– – –) the first-order approximation in Eq. (28), and (———) numerical computations.

A/cm², the fuel supply will be decreased. As this means that i_{in} decreases, this will result in an increase in the total fuel utilization, u_1. Since u_1 cannot be higher than unity the line $u_1 = 1$ represents a limit. However, for large values of u_1, the linearization of the Nernst equation fails and consequently the analytical solution intersects the line $u_1 = 1$ (as shown in Fig. 7). Since this is not possible, the analytical expression in Eq. (25) cannot be used for very small values of i_{in}. Evidently, when u_1 is almost unity and we continue to decrease i_{in}, the output current density must approximately follow the line $u_1 = 1$ down to the origin. Numerical calculations, based on the non-linearized Nernst equation, show a quite sharp transition from the curved line according to Eq. (25) to the line $u_1 = 1$. For $u_1 > 0.8$ the analytical solution starts deviating from the numerical solution, but significant deviations occur only for very high values of the total fuel utilization u_1. The analytical expression in Eq. (25) is thus very accurate up to high utilizations.

The output current density i_{out} according to Eq. (28) nearly coincides with the numerical solution up to very high values for the total fuel utilization u_1 and is therefore not plotted in Fig. 7. A close-up of the curve obtained from Eq. (28) is given in Fig. 8. This figure also gives results for the value $BLR_{load} = 5\ \Omega\ cm^2$ (bottom curves), which is a typical value for the load resistance of an MCFC at normal operation ($i_{out} = 150$–160 mA/cm²).

It is evident that optimum conditions for fuel cell operation are near the sharp transition point at which the output current density diverge from the analytical solution. Because otherwise, either fuel utilization becomes too high and the cell voltage (given by $BLR_{load} i_{out}$) drops strongly, or the utilization is too low and then not sufficient hydrogen is converted, which in general leads to a lower system efficiency. Fig. 7 also shows that the decrease in i_{out} is small up to very high values of the total utilization u_1. Hence, in principle, high utilizations can be achieved without a large decrease in cell voltage or output power density (i.e. $BLR_{load} i_{out}^2$).

7. Conclusions

The following conclusions could be drawn from the present study.

1. A simple stationary 'basic model' was developed, based on the assumptions shown in Table 1. The 'basic model' can be used to describe isothermal fuel cell behaviour, independent of the type of fuel cell.

2. It was shown that the modeling of fuel cells can be simplified by the introduction of:

- The 'equivalent input current', I_{in}, being the maximum amount of current that is produced in the case of complete fuel utilization. It can be calculated from the gas composition and the gas flow rate, using Faraday's law.
- A linear relation for the local Nernst potential as a function of the fuel utilization.

3. Linearization of the Nernst potential in the 'basic model' results in a cell model that can be solved analytically. For an MCFC the results obtained from the analytical cell model are found to be accurate up to high fuel utilizations, when compared with numerical computations based on the non-linearized Nernst equation. The analytical cell model also agrees well with measurements obtained by Machielse [1] on an isothermal 1000 cm² MCFC bench-scale cell.

4. The influence of simplified current distributions in the cell was examined: a homogeneous current density and a linearly decreasing current density were compared with a

realistic current distribution. For an MCFC the loss in cell voltage corresponding with a homogeneous current distribution is almost 10 mV lower than the actual loss in cell voltage.

5. The 'basic model' contains two independent variables, which means essentially that a fuel cell has two 'control knobs', i.e. the external load resistance R_{load} and the fuel supply through the equivalent input current I_{in}.

6. The analytical cell model can be used to express the cell current and the cell voltage in terms of the independent variables. Eq. (17) for the cell voltage clearly shows the overpotential due to fuel utilization. This so-called 'Nernst loss', is proportional to the fuel utilization and the slope α of the linearized Nernst equation. Eq. (25) for the cell current is analogous to Ohm's law. The influence of the Nernst loss appears as an 'utilization resistance', being proportional to the slope α and inversely proportional to the equivalent input current, I_{in}.

7. Fuel cells can deliver large peak powers, of course at the expense of losing efficiency. Compared with normal (high efficient) operation, the power output of an MCFC can be increased by about 50% by just increasing the input flow even at constant cell voltage. By also decreasing the load resistance R_{load} and consequently the cell voltage, the power output can be increased by about 100%.

8. Fuel cells can be operated at high utilizations without a large decrease in cell voltage or output power density.

8. List of symbols

A_1	decrease in cell voltage due to the non-homogeneity of the current distribution, V
A_2	inaccuracy in the first-order approximation, V
B	width of the rectangular cell, m
C	surface between the initial dip in $V_{eq}(u)$ and the linearized function $V^*_{eq}(u)$, V
c	molar concentration of the gas mixture, mol/m^3
F	constant of Faraday, C/mol
i	local current density, A/m^2
I_{in}	total current equivalent of the fuel supply, A
i_{in}	total current equivalent of the fuel supply per unit cell surface, A/m^2
I_{out}	total current output of a fuel cell, A
i_{out}	total current output of a fuel cell per unit cell surface; average current density, A/m^2
i_{max}	maximum output current density for a fixed value of the load resistance, A/m^2
K	equilibrium constant for concentrations in the shift reaction
L	length of the rectangular cell, m
n	total number of moles in a control volume, mol
n_i	number of moles of a species in a control volume, mol
p_{out}	output power density, W/m^2
p_i	partial pressure of the ith species in the fuel, N/m^2
r	constant quasi-ohmic resistance, Ω m^2
R_{load}	external load resistance, Ω
R	universal gas constant, J/(mol K)
T	absolute cell temperature, K
u	fuel utilization
u^*	point of inflection of the function $V_{eq}(u)$
u_1	total fuel utilization, i.e. value of u at the cell outlet
v	utilization of CO
$V_{eq}(u)$	Nernst potential as a function of the utilization u, V
$V^*_{eq}(u)$	linear fit for $V_{eq}(u)$, V
V_{cell}	cell voltage, V
V_{cor}	intercept of linearized polarization curve ($V_{cor}=0$ for the MCFC), V
V^*_{cell}	cell voltage if the Nernst equation is linear with respect to u, V
V^{ext}_{cell}	cell voltage corresponding with a partly linearized Nernst equation, V
x	scaled (i.e. relative) distance to the cell inlet
X	distance to the cell inlet, m
X_i	mole fraction of the ith species
Z	dimensionless number (see Eq. (19))

Greek letters

α	characteristic value for the derivative of $-V_{eq}(u)$ with respect to u, V
η	local overpotential, V
ζ	integration variable

Abbreviations

OCV	open-circuit voltage, i.e. $V_{eq}(0)$
MCFC	molten carbonate fuel cell
ODE	ordinary differential equation
BVP	boundary value problem

Appendix A. The equilibrium (or Nernst) potential as a function of the utilization in the case of an MCFC

In this appendix an expression for the local equilibrium potential inside an MCFC as a function of the local fuel utilization, u, is derived. The derivation is based on a common representation of the Nernst equation and on the assumptions 2, 3, 6 and 7 given in Table 1. Furthermore, we neglect diffusion effects in the gas phase, i.e. the anode gases are considered to be homogeneous over the cross section of a channel (conform to assumption 4). We also neglect the methane reforming reaction and distinguish only four chemical species in the fuel flow, i.e. H_2, CO, H_2O and CO_2. Partial properties are denoted with an index $i \in \{1,\ldots,4\}$, using the following sequence for the species

i	1	2	3	4
Species	H_2	CO	H_2O	CO_2

The cell half-reaction at the anode side of an MCFC is given by

$$H_2 + CO_3^{2-} \rightarrow H_2O + CO_2 + 2e^- \quad (A1)$$

Assuming constant partial pressures for the oxidant species, the corresponding Nernst equation can be written as

$$V_{eq}(u) = V_{eq}(0) - \frac{RT}{2F}\ln\frac{p_1(0)}{p_3(0)p_4(0)} + \frac{RT}{2F}\ln\frac{p_1(u)}{p_3(u)p_4(u)} \quad (A2)$$

where $V_{eq}(0)$ is the OCV. The OCV can be calculated from the inlet gas compositions which are assumed to be known. If the fuel behaves like an ideal gas we can use the ideal gas law to determine the partial pressures, p_i, of the components

$$p_i = cRTX_i, \quad i = 1, \ldots, 4 \quad (A3)$$

with X_i the mole fraction of the ith species, c the molar concentration of the mixture and R the universal gas constant. Note that c is constant throughout the cell, since we assumed temperature and pressure to be uniform. Using Eq. (A3) to eliminate the partial pressures from the Nernst Eq. (A2) we obtain

$$V_{eq}(u) = V_{eq}(0) - \frac{RT}{2F}\ln\frac{X_1(0)}{X_3(0)X_4(0)} + \frac{RT}{2F}\ln\frac{X_1(u)}{X_3(u)X_4(u)} \quad (A4)$$

Hence, to express the local equilibrium potential in terms of u we have to determine the mole fractions X_i as functions of u.

To this end, the number $n_i(0)$, $(i = 1,\ldots,4)$ is defined as the number of moles of the ith species that enters the cell at the anode side per unit of time. The total number of moles $n(0)$ that enters at the anode side, per unit of time, is given by the sum of $n_i(0)$ over all i. The numbers $n_i(u)$ and $n(u)$ are defined in an analogous way and are related to one and the same volume element, following the motion of the flow. The mole fractions of the species as a function of the utilization can be written as

$$X_i(u) = \frac{n_i(u)}{n(u)}, \quad i = 1, \ldots, 4 \quad (A5)$$

The numbers $n_i(u)$ in Eq. (A5) depend not only on the conversion of hydrogen by the electrochemical reaction, but also on the production of hydrogen due to the water–gas shift reaction

$$CO + H_2O \rightleftharpoons CO_2 + H_2 \quad (A6)$$

The total number of moles H_2 that can be converted by the electrochemical reaction in the case of complete fuel utilization is equal to the number of moles H_2 and CO that enters the cell. Since the utilization $u(x)$ is defined as the fraction of this supply that is converted in the interval $[0,x]$ we have

$$n_1(u) + n_2(u) = (n_1(0) + n_2(0))(1 - u) \quad (A7)$$

The total number of moles CO that is converted by the shift reaction if complete fuel utilization is achieved is given by $n_2(0)$. The fraction of this number that is converted between the cell inlet and the position that corresponds with the utilization u, is denoted by $v(u)$. Hence, by the definition of v we also have

$$n_2(u) = n_2(0)(1 - v(u)) \quad (A8)$$

Below, the mole fractions X_i, as given by Eq. (A5), are expressed in terms of u and $v(u)$. The equilibrium potential in terms of u and $v(u)$ follows from the representation of the Nernst equation in Eq. (A4). Next, the equilibrium condition for the shift reaction is used to determine v as a function of u, after which the equilibrium potential can be expressed in terms of u only.

In order to determine the mole fractions as functions of u and $v(u)$ we first subtract Eq. (A8) from Eq. (A7), yielding

$$n_1(u) = n_1(0) - (n_1(0) + n_2(0))u + n_2(0)v(u) \quad (A9)$$

The second term in the right-hand side of Eq. (A9) gives the decrease in the number $n_1(u)$ due to the electrochemical reaction. Hence, from the reaction Eq. (A1) it follows that in the control volume $(n_1(0) + n_2(0))u$ moles CO_2 and as many moles H_2O are produced by the electrochemical reaction. The last term in Eq. (A9) is equal to the number of moles H_2 produced by the shift reaction. From the reaction in Eq. (A6) it follows that in the control volume $n_2(0)v(u)$ moles CO_2 are produced and as many moles H_2O are converted by the shift reaction. Hence, the numbers $n_3(u)$ and $n_4(u)$ are given by, respectively

$$n_3(u) = n_3(0) + (n_1(0) + n_2(0))u - n_2(0)v(u)$$

$$n_4(u) = n_4(0) + (n_1(0) + n_2(0))u + n_2(0)v(u) \quad (A10)$$

The total number of moles in the control volume can now be calculated by adding the numbers n_i

$$n(u) = \sum_{i=1}^{4} n_i(u) = n(0)(1 + [X_1(0) + X_2(0)]u) \quad (A11)$$

Using the identities in Eqs. (A5), (A7)–(A11) and the following notation

$$a_i = \frac{X_i(0)}{X_2(0)}, \quad b = \frac{X_1(0) + X_2(0)}{X_2(0)} = 1 + a_1,$$

$$\phi(u) = 1 + (X_1(0) + X_2(0))u \quad (A12)$$

The mole fractions in Eq. (A5) can be written as

$$X_1(u) = X_1(0)\left(1 - \frac{1}{a_1}(bu - v)\right)\Big/\phi(u),$$

$$X_2(u) = X_2(0)(1 - v)/\phi(u)$$

$$X_3(u) = X_3(0)\left(1 + \frac{1}{a_3}(bu - v)\right)\Big/\phi(u)$$

$$X_4(u) = X_4(0)\left(1+\frac{1}{a_4}(bu+v)\right)\Big/\phi(u) \qquad \text{(A13)}$$

We assume that the water–gas shift reaction in the MCFC is in equilibrium throughout the cell. Using the identities in Eq. (A3) or Eq. (A12), the equilibrium constant K for to the reverse shift reaction can be rewritten as, respectively

$$K=\frac{p_2p_3}{p_1p_4}=\frac{X_2(0)X_3(0)}{X_1(0)X_4(0)}=\frac{X_2(u)X_3(u)}{X_1(u)X_4(u)}$$

or

$$K=\frac{a_3}{a_1a_4}$$

Substitution of the expressions for the mole fractions (Eq. (A13)) into the equilibrium condition yields

$$(1-v)\left(1+\frac{1}{a_3}(bu-v)\right) = \left(1-\frac{1}{a_1}(bu-v)\right)\left(1+\frac{1}{a_4}(bu+v)\right) \qquad \text{(A14)}$$

Solving Eq. (A14) for $v(u)$ and using the equilibrium condition again, we find

$$v(u)=d+\frac{b}{2(1-K)}u - \sqrt{\left(d-\left(1-\frac{1}{2(1-K)}\right)bu\right)^2+\frac{(2Ka_1+a_3)b}{1-K}u}, \qquad (0<K<1) \qquad \text{(A15)}$$

where the trivial condition $v(0)=0$ is satisfied and d is a constant defined by

$$d=\frac{1+a_3+K(a_1+a_4)}{2(1-K)}$$

Using Eqs. (A13) the Nernst Eq. (A4), for zero oxidant utilization, can finally be rewritten in terms of u

$$V_{eq}(u)=V_{eq}(0)+\frac{RT}{2F}\left[\ln\left(1-\frac{1}{a_1}(bu-v(u))\right)+\ln\phi(u) - \ln\left(1+\frac{1}{a_3}(bu-v(u))\right)-\ln\left(1+\frac{1}{a_4}(bu+v(u))\right)\right] \qquad \text{(A16)}$$

utilizing for $\phi(u)$ and $v(u)$ the expressions given by Eqs. (A12) and (A15), respectively.

In an analogous way, the obtained expression for $V_{eq}(u)$ can be extended to an expression that also accounts for the utilization of oxidant. However, this latter step is also described in Ref. [4] and has been omitted in this paper.

A.1. Nota bene

Fig. 9 shows an example of the reaction coordinate $v(u)$ for the conversion of CO by the shift reaction. For small values of the fuel utilization, CO is produced from the reverse shift reaction, while when the hydrogen partial pressure becomes low, the shift reaction evolves towards the decomposition of the produced CO. The value of $u>0$ for which v is equal to zero is obtained by setting $v=0$ in Eq. (A14) and solving the result for u

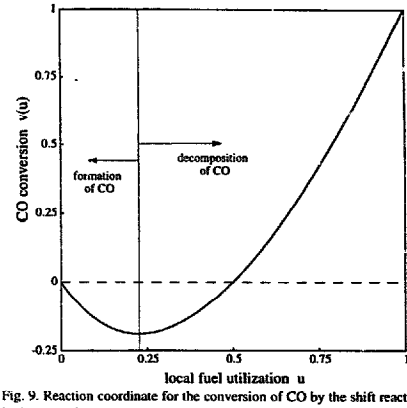

Fig. 9. Reaction coordinate for the conversion of CO by the shift reaction, in the case of standard gas compositions (see Table 2).

$$u=1-\frac{(1+1/K)X_2(0)+X_4(0)}{X_1(0)+X_2(0)} \Rightarrow v(u)=0$$

This value is exactly 0.5 for the standard gas compositions (see Table 2) and $K=0.5$.

Appendix B. Cell voltage as a function of the total utilization

In Eq. (15) the cell voltage V^*_{cell} in the solution of the analytical cell model was written as the average value of the linearized equilibrium potential minus the polarization losses due to the quasi-ohmic resistance, r. In the same way Eq. (15) was derived, but starting with the ODE in the BVP, it can be shown that the cell voltage V_{cell} in Section 2 can be written as

$$V_{cell}=\frac{1}{u_1}\int_0^{u_1}V_{eq}(u)\,du-\frac{r}{i_{out}}\int_0^1 i^2(x)\,dx \qquad \text{(A17)}$$

In Section 4.1, it was shown (see Fig. 3) that the initial dip in the Nernst equation has a very small influence on the current distribution inside the cell. Hence, at normal operation, the second integral in Eq. (A17) can still be approximated using a constant (zero-order) or linear (first-order) approximation for the current distribution inside the cell, just as in the reduction of Eq. (15). Using the first-order approximation, Eq. (A17) can be reduced to

$$V_{cell} \approx \frac{1}{u_1}\int_0^{u_1} V_{eq}(u)\,du - \left(1+\frac{1}{3}Z^2\right) r i_{out},$$

first-order approximation (A18)

Assuming that $V^*_{eq}(u)$, see Section 3, is an accurate approximation of $V_{eq}(u)$ for values of u in the interval (u^*,u_1), we set $V_{eq}(u)$ in Eq. (A18) equal to $V^*_{eq}(u)$ for values of $u > u^*$. In this way we obtain the following expression for the cell voltage

$$V_{cell} \approx V^*_{eq}(0) - \frac{1}{2}\alpha u_1 - \left(1+\frac{1}{3}Z^2\right) r i_{out} + C\frac{1}{u_1}, \quad u_1 > u^* \tag{A19}$$

where C is the surface between the initial dip in the equilibrium potential and the linear fit $V^*_{eq}(u)$

$$C = \int_0^{u^*} \{V_{eq}(u) - V^*_{eq}(u)\}\,du$$

The approximation in Eq. (A19) is also valid for values of $u_1 < u^*$, as long as $V^*_{eq}(u)$ is an accurate approximation of $V_{eq}(u)$ for values of u in the interval (u_1,u^*). Hence, Eq. (A19) is valid for values of u_1 in the interval for which the linear approximation $V^*_{eq}(u)$ is accurate.

References

[1] L.A.H. Machielse, Simple model for the estimation of isothermal fuel cell performance, *Proc. Modeling of Batteries and Fuel cells, 1991 Fall Meeting, Phoenix, AZ, USA*. Proc. Vol. 91-10. The Electrochemical Society, Pennington, NJ, USA, pp. 166–174.

[2] K. Hemmes, Computer algebra applied in electrochemistry and fuel cell modeling, *Proc. Modeling of Batteries and Fuel cells, 1991 Fall Meeting, Phoenix, AZ, USA*. Proc. Vol. 91-10. The Electrochemical Society, Pennington, NJ, USA, pp. 281–294.

[3] H.A. Liebhafsky and E.J. Cairns, *Fuel Cells and Fuel Batteries*, Wiley, New York, 1968, Appendix A.

[4] J.H. Hirschenhofer, D.B. Stauffer and R.R. Engleman, *Fuel Cells. A Handbook*, US Department of Energy, 1994, Fig. 2.4, Ch. 4, Appendix 9.2.

[5] K.R. Plowman, Y.J. Regh, P.J. Nandapurkar, R.D. Door and R.D. Mussell, Targets and progress toward improved membrane electrode assemblies for PEM fuel cells, *Ext. Abstr., Fuel Cell Seminar 1994, 28 Nov.–1 Dec 1994, San Diego, CA, USA*, pp. 470–473.

[6] A.J. Appleby and F.R. Foulkes, *Fuel Cell Handbook*, Van Nostrand Reinhold, New York, 1989, Ch. 17, p. 551.

[7] J.R. Anderson and M. Boudart (eds.), *Catalysis Science and Technology 5*, Springer, Berlin, 1984.

[8] T.L. Wolf and G. Wilemski, *J. Electrochem. Soc., 130* (1983) 48.

[9] E. Kreyszig, *Introductory Functional Analysis with Applications*, Wiley, New York, 1978, Ch. 9.

[10] K. Hemmes, F. Standaert, N. Woudstra and J.H.W. de Wit, Fundamentals of fuel cells and fuel cell modeling, *Proc. 2nd Int. Fuel Cell Conf. (IFCC), Kobe, Japan, 5–8 Febr. 1996*, pp. 389–992.